

ISTITUTO NAZIONALE DI FISICA NUCLEARE

Sezione di Trieste

INFN/AE-94/29

16 dicembre 1994

F. Tassarotto

RESULTS ON THE SPIN DEPENDENT STRUCTURE FUNCTIONS OF THE PROTON

RESULTS ON THE SPIN DEPENDENT STRUCTURE FUNCTIONS OF THE PROTON

FULVIO TESSAROTTO

*Istituto Nazionale di Fisica Nucleare, Sezione di Trieste,
Area di Ricerca, Padriciano 99, 34012 Trieste, Italy*

on behalf of the Spin Muon Collaboration (SMC)

ABSTRACT

The spin-dependent structure functions of the proton g_1^p and g_2^p have recently been measured in inclusive polarised muon scattering by the SMC at CERN. The first moment of g_1^p has been estimated at $Q^2 = 10 \text{ GeV}^2$ to be $\Gamma_1^p = 0.136 \pm 0.011(\text{stat.}) \pm 0.011(\text{syst.})$, in disagreement with the Ellis-Jaffe prediction: $\Gamma_{E.J.}^p = 0.176 \pm 0.006$. Using all published data on g_1 of the proton, the neutron and the deuteron a confirmation of the Bjorken sum rule at the 10% accuracy level was achieved and estimates of the quark spin contribution to the nucleon spin $\Delta\Sigma \approx 0.30$ were obtained.

1 Polarised Deep Inelastic Scattering

1.1 The Structure Functions

Most of the present knowledge on the internal structure of the nucleon rests on the extensive experimental information obtained in deep inelastic scattering (DIS) experiments using high-energy charged and neutral lepton beams.

The cross-section formula for high energy charged leptons DIS interaction on nucleons is obtained, in the single photon exchange approximation, from the product of a leptonic tensor $L_{\mu\nu}$ and a hadronic tensor $H^{\mu\nu}$. The latter can be expanded into Lorentz covariant terms whose coefficients define the structure functions to be measured.

There are four such independent structure functions: $F_1(x, Q^2)$, $F_2(x, Q^2)$, $g_1(x, Q^2)$ and $g_2(x, Q^2)$, where the kinematical variables are the Bjorken scaling variable x and the negative squared four-momentum transfer Q^2 .

F_1 and F_2 come from the symmetric part $H_S^{\mu\nu}$ and are independent of the nucleon spin, while g_1 and g_2 come from the antisymmetric term $H_A^{\mu\nu}$ dependent on the nucleon spin.

Only F_1 and F_2 can be measured in unpolarised DIS experiments, while both polarised beam and polarised target are needed to experimentally access g_1 or g_2 , since

$$L_{\mu\nu} H^{\mu\nu} = L_{\mu\nu}^S H_S^{\mu\nu} + L_{\mu\nu}^A H_A^{\mu\nu} \quad (1)$$

and $L_{\mu\nu}^A$ vanishes for unpolarised leptons.

Denoting the parallel (antiparallel) polarisation of the target nucleon spins with respect to the one of the incident lepton by $\uparrow\uparrow$ ($\uparrow\downarrow$), the spin-averaged cross-section: $2\bar{\sigma} = \sigma^{\uparrow\downarrow} + \sigma^{\uparrow\uparrow}$ is obtained from $L_{\mu\nu}^S H_S^{\mu\nu}$, and is given by:

$$\frac{d\bar{\sigma}}{dx dQ^2} = \frac{4\pi\alpha^2}{xQ^4} \left[\left(1 - \frac{Q^2}{2ME x} - \frac{Q^2}{4E^2} \right) F_2(x, Q^2) + \frac{Q^4}{4M^2 E^2 x} F_1(x, Q^2) \right] \quad (2)$$

while the spin-dependent part of the cross-section: $2\Delta\sigma = \sigma^{\uparrow\downarrow} - \sigma^{\uparrow\uparrow}$ is obtained from $L_{\mu\nu}^A H_A^{\mu\nu}$:

$$\frac{d\Delta\sigma}{dx dQ^2} = \frac{2\pi\alpha^2}{ME x Q^2} \left[\left(2 - \frac{Q^2}{2ME x} - \frac{Q^2}{4E^2} \right) g_1(x, Q^2) - \frac{2Mx}{E} g_2(x, Q^2) \right]. \quad (3)$$

The function g_1 is expected to show scaling behaviour similar to F_1 and F_2 , i.e. $g_1(x, Q^2) \rightarrow g_1(x)$ for $Q^2 \rightarrow \infty$.

In the framework of the Quark Parton Model (QPM) g_1 has a very simple interpretation, similar to the one of the structure function F_1 :

$$g_1(x) = \frac{1}{2} \sum_i e_i^2 [q_i^+(x) - q_i^-(x)], \quad F_1(x) = \frac{1}{2} \sum_i e_i^2 [q_i^+(x) + q_i^-(x)] \quad (4)$$

where q_i^+ (q_i^-) denotes the distribution function of quarks and antiquarks of flavour i having their spin parallel (antiparallel) to the nucleon spin and e_i is the corresponding electric charge.

The structure function g_2 can be written as a sum of a contribution, g_2^{ww} , directly calculable from g_1 , and a pure twist-3 term¹ \bar{g}_2 :

$$g_2(x, Q^2) = g_2^{ww}(x, Q^2) + \bar{g}_2(x, Q^2), \quad g_2^{ww}(x, Q^2) = -g_1(x, Q^2) + \int_x^1 g_1(t, Q^2) \frac{dt}{t}. \quad (5)$$

There is no simple interpretation of g_2 in the QPM, since \bar{g}_2 describes quark-gluon correlations, which are not present in the simple versions of the QPM.

1.2 Sum Rules

Although the explicit form of the structure functions is not predicted by theory, there are, in some cases, definite predictions for their moments, which are called sum rules. In particular the first moments of g_1 :

$$\Gamma_1(Q^2) = \int_0^1 g_1(x, Q^2) dx \quad (6)$$

are expected to obey the most important and fundamental sum rule for polarised DIS, the Bjorken sum rule, which was first derived² from current algebra in 1966 and has been refined by including perturbative QCD corrections:

$$\Gamma_1^p(Q^2) - \Gamma_1^n(Q^2) = \frac{1}{6} \frac{G_A}{G_V} C_{NS}(Q^2) \quad (7)$$

The labels p and n refer to proton and neutron, G_A and G_V are the weak decay axial and vector coupling constants, C_{NS} is the perturbative non-singlet coefficient function which has been calculated³ up to order-3 in α_s . In the Bjorken limit:

$$\Gamma_1^p - \Gamma_1^n = \frac{1}{6} \frac{G_A}{G_V} = \frac{1}{6} (F + D) \quad (8)$$

where $(F + D)$ is the matrix element of the triplet current. This current is conserved and therefore scale independent and it is equal to the axial coupling measured in neutron β decay: $(F + D) = 1.2573 \pm 0.0028$.

Assuming that $SU(3)_f$ symmetry is valid for the baryon octet and that the strange quark sea in the nucleon is unpolarised, Ellis and Jaffe⁴ have derived separate predictions (E.J. sum rules) for Γ_1^p and Γ_1^n relating them to the matrix elements of the octet current, which is also a conserved quantity.

Releasing the assumption on the strange sea polarisation from the E.J. sum rules, one can derive a relation between $\Gamma_1^{p,n}$ and $\Delta\Sigma$, which is valid in the Bjorken limit and for the three lightest quark flavours:

$$\Gamma_1^{p,n} = \pm \frac{1}{12}(F + D) + \frac{1}{36}(3F - D) + \frac{1}{9}\Delta\Sigma \quad (9)$$

The most recent fit from octet decay data⁵ gives: $(3F - D) = 0.579 \pm 0.025$.

Using Eq. 4, one can see that in the framework of the QPM:

$$\Delta\Sigma = \Delta u + \Delta d + \Delta s, \quad \Delta q = \int_0^1 \{q_i^+(x) - q_i^-(x)\} dx, \quad q = u, d, s. \quad (10)$$

i.e. $\Delta\Sigma$ represents the fraction of the nucleon helicity carried by the quarks, which enters the total nucleon spin equation:

$$\frac{1}{2} = \frac{1}{2}\Delta\Sigma + \Delta G + \langle L_z \rangle \quad (11)$$

where ΔG is the helicity carried by gluons and $\langle L_z \rangle$ is the contribution from the partons orbital angular momentum. If $\Delta s = 0$, as in the E.J. sum rule, the QPM expected value for $\Delta\Sigma$ is $(3F - D) \approx 0.58$; otherwise: $\Delta\Sigma = 0.58 + 3\Delta s$.

A sum rule for the structure function g_2 has been derived by Burkhardt and Cottingham⁶ using Regge theory:

$$\int_0^1 g_2(x, Q^2) dx = 0 \quad (12)$$

but the validity of the derivation is presently being questioned¹.

1.3 Extraction of g_1

Experimentally, g_1 is extracted from measured asymmetries obtained using longitudinally polarised beam and target. Data are collected in the two relative spin orientations and the observed counting rate asymmetry Δ is given by:

$$\Delta = \frac{N^{\uparrow\downarrow} - N^{\uparrow\uparrow}}{N^{\uparrow\downarrow} + N^{\uparrow\uparrow}} = P_b P_t f A \quad (13)$$

From Δ one can deduce the lepton-nucleon cross-section asymmetry $A = \Delta\sigma/\bar{\sigma}$ provided one knows the beam polarisation P_b , the target polarisation P_t , and the dilution factor f (fraction of polarisable nucleons).

A is related to the virtual-photon nucleon absorption cross-section asymmetry $A_1(x, Q^2)$ by:

$$A(x, Q^2) = D(x, Q^2) [A_1^p(x, Q^2) + \eta(x, Q^2)A_2(x, Q^2)] \approx D(x, Q^2)A_1^p(x, Q^2) \quad (14)$$

where the photon depolarisation function $D(x, Q^2)$ depends also on the unpolarised structure function $R(x, Q^2)$ which represents the ratio between the longitudinally and the transversely polarised photon absorption cross-section. The approximate equality holds since the kinematical factor η is small in the range covered by present experiments. The structure function g_1 can then be extracted from A_1 using the values of F_1 determined from other experiments:

$$g_1(x, Q^2) = A_1(x, Q^2)F_1(x, Q^2). \quad (15)$$

1.4 Earlier Results

First measurements of g_1^p were performed at SLAC by Experiments E80⁷ and E130⁸ and at CERN by the European Muon Collaboration (EMC)⁹. These data showed an important deviation from the *E.J.* prediction implying the total quark spin contribution to the spin of the nucleon to be small: $\Delta\Sigma = 0.12 \pm 0.16$. Several theoretical ideas were proposed in order to understand this result, and new experiments were prepared to collect polarised DIS data at CERN, SLAC and DESY.

2 The Spin Muon Collaboration measurement of g_1^p

2.1 The Measurement of g_1^d

During 1991 and 1992 The Spin Muon Collaboration Experiment collected inclusive DIS data using a polarised deuterated butanol target to perform the first measurement of the structure function g_1^d . The CERN SPS 100 GeV positive muon beam was used and the accessed kinematical range was $0.006 < x < 0.6$, $1 \text{ GeV}^2 < Q^2 < 30 \text{ GeV}^2$. The result¹⁰ for the integral of g_1^d was: $\Gamma_1^d = 0.023 \pm 0.020(\text{stat}) \pm 0.015(\text{syst.})$, smaller than the prediction of the *E.J.* sum rules. Combining the SMC data with earlier measurements of g_1^p the difference $\Gamma_1^p - \Gamma_1^n$ was extracted for the first time and found to be in agreement with the Bjorken Sum Rule. High-statistics data on g_1^n from polarised e^- -³He scattering were reported¹¹ by Experiment E142 at SLAC, and a combined analysis¹² of SMC and E142 data showed full consistency between the data in the kinematic region of overlap, and emphasized that the conclusions concerning Γ_1 are very sensitive to the small x extrapolation of g_1 and to higher order QCD corrections.

2.2 The Muon Beam

The positive muon beam used for the measurement of g_1^p in 1993 was provided by the CERN SPS and had an average energy of 190 GeV; the intensity was $\approx 4 \times 10^7$ muons/spill, with a spill time of 2.4 s and a period of 14.4 s. The beam was polarised due to the parity-violating meson decays from which it was produced; its polarisation P_μ was measured by the SMC muon polarimeter¹³ to be $P_\mu = -0.803 \pm 0.029(\text{stat.}) \pm 0.020(\text{syst.})$ by fitting the shape of the energy spectrum of positrons from muon decay $\mu^+ \rightarrow e^+ \nu_e \bar{\nu}_\mu$. This value of P_μ was in good agreement with Monte Carlo simulations

of the beam transport¹⁴. The momentum of the incident muon was measured event by event using a bending magnet upstream of the target.

2.3 The SMC Polarised Target

The target used for the measurement of g_1^p consisted of two 60 cm long, 5 cm diameter cells, separated by 30 cm. The material was butanol (plus about 5% H₂O) doped with paramagnetic complexes and frozen into ~ 1.5 mm diameter beads. The cells were inside a ³He/⁴He dilution refrigerator at a temperature of 0.3 K when polarising and below 60 mK in frozen-spin operation. A 2.5 T field aligned along the beam axis was provided by a superconducting solenoid and was homogeneous at a level of 2×10^{-5} throughout the target volume.

Unbound protons were polarised by dynamic nuclear polarisation induced by microwave power, in opposite direction in the two target cells. Ten coils along the target were used to measure the polarisation P_T via NMR signals, which were calibrated by comparison to the thermal equilibrium signals around 1 K. The average P_T was 0.86 and the relative accuracy of the measurement was 3%. The spin directions were reversed by spin rotation every 5 hours. The dilution factor f , i.e. the fraction of event yield from polarised protons in the target, was on average $f \simeq 0.12$.

2.4 The Spectrometer and the Analysis

Upstream of the target a set of scintillator hodoscopes and proportional chambers were used to reconstruct the incident muon track. Downstream of the target a spectrometer consisting of a conventional large-aperture dipole magnet and proportional chambers, drift chambers and streamer tubes (a total of 150 planes), was used to reconstruct the trajectory and to measure the momentum of the scattered muon. Scintillator hodoscopes, located downstream of a 2 m thick iron hadron absorber were used to identify the scattered muons and to provide the triggering signal.

The average resolution on the reconstructed interaction vertex was 30 mm along the beam direction and 0.3 mm perpendicular to the beam direction. Cuts were applied to minimize smearing effects, to limit the size of radiative corrections, to reject muons originated from decays in the target, to equalize the beam illumination of the two target cells and to ensure proper separation of upstream and downstream cell interaction vertices. After cuts, the data sample amounted to 4.4×10^6 events in the kinematical range $0.003 < x < 0.7$ and $1 \text{ GeV}^2 < Q^2 < 60 \text{ GeV}^2$.

The virtual-photon absorption asymmetry A_1^p was obtained from the measured asymmetry A neglecting the A_2 term of Eq. 14. An important reduction of the contribution to the systematic error coming from the A_2 term was obtained from the direct measurement of A_2 .

A_1^p was extracted from combinations of data sets taken before and after a polarisation reversal, weighting each event with the corresponding values of the photon depolarisation D and the dilution factor f . The advantage of simultaneous data taking with two oppositely polarised cells is the cancellation of systematic errors due to the luminosities and the acceptances, provided that the ratio between the upstream

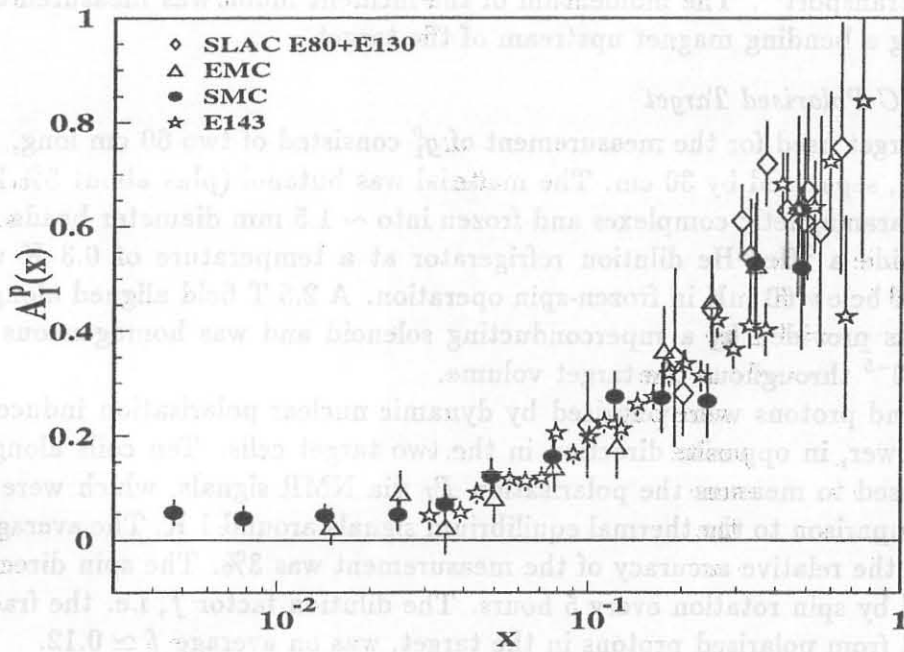


Figure 1: The virtual-photon proton cross section asymmetry A_1^P as a function of x . The errors shown are statistical only

target cell acceptance and the downstream one remains constant within two polarisation reversals. The time dependence of all detector efficiencies was extensively studied and included in the systematic error on A . The effect of spin-dependent radiative corrections was calculated and taken into account.

2.5 The Asymmetry A_1^P

The SMC measured values of A_1^P have recently been published¹⁵. They are presented in Fig. 1 as function of x . The mean Q^2 of the SMC data points varies with increasing x from 1.3 to 58 GeV². Also shown are the earlier data from E80⁷, E130⁸, the EMC⁹, and the recent results from E143 SLAC experiment¹⁶. This figure shows the consistency of the data from SMC and E143 and their complementarity: E143 has performed a high statistics measurement in the region of $x > 0.03$ while the SMC has a unique capability to explore the very low x region.

2.6 The Measurement of A_2

The Spin Muon Collaboration has also performed the first measurement of A_2^P , in a dedicated experiment¹⁷ where a 100 GeV muon beam was used and the proton polarisation was held in a direction perpendicular to the beam by a 0.5 T dipole field. A total of 8.7×10^5 events was obtained in the range $0.006 < x < 0.6$ and $1 < Q^2 < 30$ GeV². The results are shown in Fig. 2: A_2 was found to be significantly smaller than its positivity limit \sqrt{R} (with $R(x, Q^2)$ taken from the SLAC parametrization¹⁹), and consistent with the values obtained with $\bar{g}_2 = 0$ in Eq. 5.

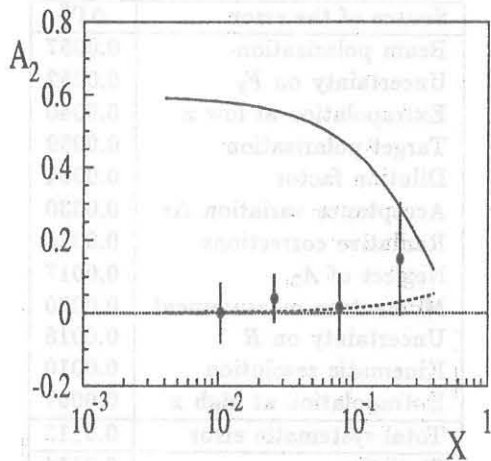


Figure 2: The asymmetry A_2 as a function of x . The solid line shows the positivity limit and the dashed line shows a prediction without the $\overline{g_2}$ contribution.

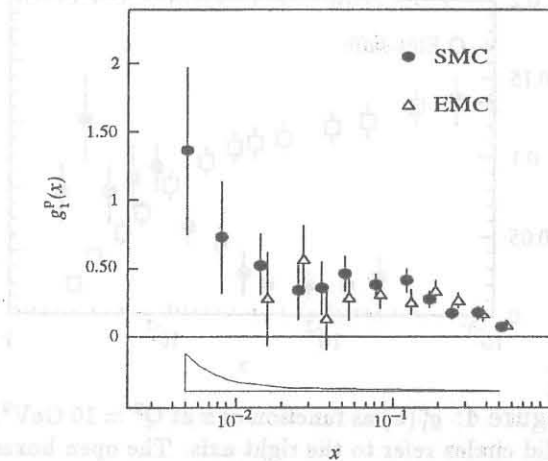


Figure 3: The spin dependent structure function $g_1^p(x)$. Error bars represent the statistical uncertainty. The size of the systematic errors for the SMC data is indicated by the shaded area.

2.7 The Structure Function g_1^p

The structure function g_1^p has been extracted from A_1^p at each x bin using Eq. 15 and the relation:

$$F_1(x, Q^2) = \frac{F_2(x, Q^2)}{2x [1 + R(x, Q^2)]} \quad (16)$$

where the unpolarised structure function $F_2(x, Q^2)$ was taken from the parametrization provided by NMC¹⁸ and the function $R(x, Q^2)$ was taken from a global fit¹⁹ of SLAC data.

In Fig.3 the result for $g_1^p(x)$ is presented together with the EMC data, recalculated using the NMC parametrization¹⁸ for F_2 . The rise at low x is interesting although not significant enough to question the usually expected Regge behaviour²⁰. Recent papers^{5,21} however suggest the possibility of singular behavior of $g_1(x)$ at small x .

2.8 Estimate of Γ_1^p

To evaluate the integral $\Gamma_1^p(Q^2)$ (Eq. 6) at a fixed Q_0^2 , the values of g_1^p in each bin need to be recalculated at Q_0^2 before integration. This was done using $F_1(x, Q_0^2)$ in Eq. 15 and assuming that A_1 does not depend on Q^2 . This assumption is consistent with the data and with recent theoretical calculations²², however it might not be valid in the low x region where the data are not precise enough to exclude larger scaling violation of A_1 . SMC has chosen $Q_0^2 = 10 \text{ GeV}^2$, which represents an average value for the data. The values of $g_1^p(x, Q_0^2)$ are shown in Fig.4 as solid circles. Integrating over the measured x range one obtains:

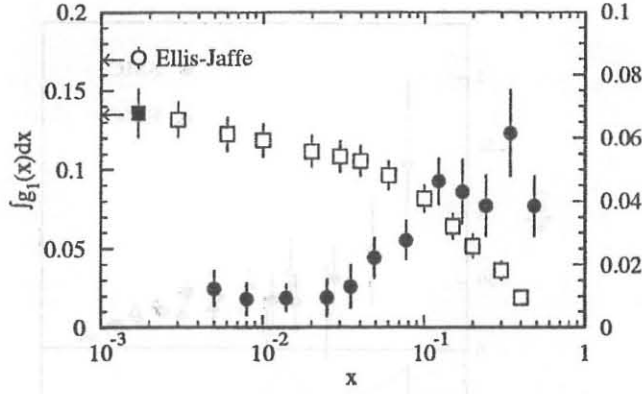


Figure 4: $g_1^p(x)$ as function of x at $Q^2 = 10 \text{ GeV}^2$. The solid circles refer to the right axis. The open boxes (left axis) show the partial integral in x from the lower edge of the bin to 1 of g_1^p . Only statistical errors are shown. The solid square is the SMC result for Γ_1^p with statistical and systematic errors combined in quadrature. Also shown is the prediction from Ellis-Jaffe sum rule.

Source of the error	$\Delta\Gamma_1^p$
Beam polarization	0.0057
Uncertainty on F_2	0.0052
Extrapolation at low x	0.0040
Target polarization	0.0039
Dilution factor	0.0034
Acceptance variation Δr	0.0030
Radiative corrections	0.0023
Neglect of A_2	0.0017
Momentum measurement	0.0020
Uncertainty on R	0.0018
Kinematic resolution	0.0010
Extrapolation at high x	0.0007
Total systematic error	0.0113
Statistics	0.0114

Table I. Contributions to the systematic error of Γ_1^p

$$\int_{0.003}^{0.7} g_1^p(x, Q_0^2) dx = 0.131 \pm 0.011 \pm 0.011. \quad (17)$$

where the first error is statistical and the second is systematic.

For the range $0.7 < x < 1$ the assumption that $A_1^p = 0.7 \pm 0.3$ was made and the relative contribution to the integral was estimated to be 0.0015 ± 0.0007 . Using this estimate and the g_1 points of Fig. 4 one can compute for each x bin the integral of g_1 from the minimum x value of that bin to $x = 1$: the results are shown in the same figure as open boxes.

The unmeasured range $0 < x < 0.003$ contributes to the integral g_1^p and to its error more than the high x region. In this region, the SMC assumed $g_1^p(x) = C$, which is consistent with the expected Regge behavior²⁰: $g_1^p(x) \propto x^\alpha$, with $0 < \alpha < 0.5$. The value of C was obtained from the fit of the two lowest points and the corresponding contribution to Γ_1^p amounts to 0.004 ± 0.004 . The final result for Γ_1^p at $Q_0^2 = 10 \text{ GeV}^2$ is:

$$\Gamma_1^p(Q_0^2) = 0.136 \pm 0.011 \pm 0.011 \quad (18)$$

where the first error is statistic and the second systematic. This result is represented by the closed box on Fig.4. The *E.J.* prediction is also shown in the figure as an open circle: it is more than two standard deviations above the measured value. The sources of the quoted systematic error are listed together with their contribution in Tab. 1.

3 The Spin Structure of the Nucleon

3.1 Test of the Bjorken sum Rule

The integral Γ_1^p has been recalculated for $Q_0^2 = 5 \text{ GeV}^2$ in order to test the Bjorken sum rule together with the data from E80, E130, EMC and E142.

To extract Γ_1^n from g_1^d or g_1^{He} , which are the measured structure functions, one needs to take into account nuclear effects. In the case of the deuteron data the relation is: $\Gamma_1^p + \Gamma_1^n \simeq 2\Gamma_1^d / (1 - 1.5\omega_D)$ where ω_D is the probability of the deuteron to be in a D-state. For ${}^3\text{He}$ the formula is: $\Gamma_1^n = (1.15 \pm 0.02) \Gamma_1^{He} + (0.057 \pm 0.009) \Gamma_1^p$. In this procedure the nuclear effects from shadowing and also from the Fermi motion are not taken into account.

The measured value at $Q_0^2 = 5 \text{ GeV}^2$ is $\Gamma_1^p - \Gamma_1^n = 0.204 \pm 0.029$, to be compared with the theoretical value from Eq.7 0.185 ± 0.004 , which includes perturbative QCD corrections³ up to third order in α_s , but no higher twists contributions. This provides a confirmation of the Bjorken sum rule at the one standard deviation level, corresponding to an accuracy of 10% of the predicted value.

3.2 Extraction of $\Delta\Sigma$

The quantity $\Delta\Sigma$, defined in Eq.9, is related to the matrix element of the flavour singlet fermionic axial current j_5^μ of the target:

$$j_5^\mu = \sum_{i=1}^{N_f} \bar{\psi}_i \gamma_\mu \gamma_5 \psi_i, \quad \langle p, s | j_5^\mu | p, s \rangle = M s^\mu \Delta\Sigma \quad (19)$$

where p^μ , M and s^μ are the target four-momentum, mass and spin. The current j_5^μ is not conserved, and hence $\Delta\Sigma$ is not a conserved quantum number²³. Indeed, at finite Q^2 Eq.9 becomes

$$\Gamma_1^p(Q^2) = C_{NS}(Q^2) \left[\frac{1}{12}(F + D) + \frac{1}{36}(3F - D) \right] + C_S(Q^2) \left[\frac{1}{9} \Delta\Sigma(Q^2) \right] \quad (20)$$

where, apart from the perturbative coefficient functions C_{NS} and C_S , $\Delta\Sigma$ itself is scale-dependent. In order to compare $\Delta\Sigma$ from data at different Q^2 an asymptotic value $\Delta\Sigma(\infty)$ is defined²⁴:

$$\Delta\Sigma(Q^2) = \left[1 + \frac{2}{3} \left(\frac{\alpha_s(Q^2)}{\pi} \right) + 1.2130 \left(\frac{\alpha_s(Q^2)}{\pi} \right)^2 + \dots \right] \Delta\Sigma(\infty) \quad (21)$$

From the SMC g_1^p measurement¹⁵ one extracts $\Delta\Sigma = 0.22 \pm 0.10 \pm 0.10$ and $\Delta s = -0.12 \pm 0.04 \pm 0.04$, which confirm the indications from the EMC and from the SMC g_1^d measurement that only a small fraction of the nucleon helicity is coming from the helicity of the quarks.

The experiment E142 had reported $\Delta\Sigma = 0.57 \pm 0.11$, but the value was obtained at $Q^2 = 2 \text{ GeV}^2$ without higher order QCD corrections: a combined analysis of data from E80, E130, EMC, SMC (g_1^d) and E142 gave the result $\Delta\Sigma = 0.24 \pm 0.23$. The E143 has recently quoted¹⁶ the value $\Delta\Sigma = 0.29 \pm 0.10$.

A rather consistent picture is emerging from the new data, and the understanding of the nucleon spin structure will certainly benefit from the present extensive experimental effort. Two recent publications^{25,26} have reported results from fits on all published data (including E143), where the Bjorken sum rule was taken for granted and used to estimate the strong coupling constant α_s together with $\Delta\Sigma$. Their results are in good agreement:

$$\alpha_s(M_Z) = 0.122^{+0.005}_{-0.009}, \quad \Delta\Sigma = 0.31 \pm 0.04$$

from Ref.²⁵,

$$\alpha_s(M_Z) = 0.125 \pm 0.006, \quad \Delta\Sigma = 0.33 \pm 0.04$$

from Ref.²⁶

References

- [1] R.L. Jaffe, *Comments Nucl. Part. Phys.* **19** (1990) 239.
- [2] J.D. Bjorken, *Phys. Rev.* **148** (1966) 1467; *Phys. Rev. D***1** (1970) 1376.
- [3] S.A. Larin and J.A.M. Vermaseren, *Phys. Lett.* **B259** (1991) 345.
- [4] J. Ellis and R.L. Jaffe, *Phys. Rev. D***9** (1974) 1444; *Phys. Rev. D***10** (1974) 1669.
- [5] F.E. Close and R.G. Roberts, *Phys. Lett.* **B336** (1994) 257.
- [6] H. Burkhardt and W.N. Cottingham, *Ann. Phys.* **56** (1970) 453.
- [7] SLAC E-80, M.J. Alguard et al., *Phys. Rev. Lett.* **37** (1976) 1261; *Phys. Rev. Lett.* **41** (1978) 70.
- [8] SLAC E-130, G. Baum et al., *Phys. Rev. Lett.* **51** (1983) 1135.
- [9] EMC, J. Ashman et al., *Phys. Lett.* **B206** (1988) 364.
- [10] SMC, B. Adeva et al., *Phys. Lett.* **B302** (1993) 533.
- [11] SLAC E-142, D.L. Anthony et al., *Phys. Rev. Lett.* **71** (1993) 959.
- [12] SMC, B. Adeva et al., *Phys. Lett.* **B320** (1994) 400.
- [13] SMC, B. Adeva et al., *Nucl. Instrum. Methods* **A343** (1994) 363.
- [14] N. Doble, et al., *Nucl. Instrum. Methods* **A343** (1994) 351.
- [15] SMC, D. Adams et al., *Phys. Lett.* **B329** (1994) 399.
- [16] SLAC E-143, Abe et al., preprint SLAC-PUB 6508 (Aug. 1994).
- [17] SMC, D. Adams et al., *Phys. Lett.* **B336** (1994) 125.
- [18] NMC, P. Amaudruz et al., *Phys. Lett.* **B295** (1992) 159; Errata Oct. 26, (1992) and Apr. 19, (1993).
- [19] L.W. Whitlow et al., *Phys. Lett.* **B250** (1990) 193.
- [20] R. L. Heimann, *Nucl. Phys.* **B64** (1973) 429; J. Ellis and M. Karliner, *Phys. Lett.* **B213** (1988) 73.
- [21] S.D. Bass and P.V. Landshoff, Cambridge preprint DAMTP 94/50 (1994).
- [22] G. Altarelli, P. Nason and G. Ridolfi, *Phys. Lett.* **B320** (1994) 152.
- [23] S. Forte, preprint CERN-TH 7453/94 (1994).
- [24] S.A. Larin, *Phys. Lett.* **B334** (1994) 192.
- [25] J. Ellis and M. Karliner, preprint CERN-TH 7324/94 (1994).
- [26] G. Altarelli, and G. Ridolfi, preprint CERN-TH 7415/94 (1994).